Characterization of AFLP Sequences From Regions of Maize B Chromosome Defined by 12 B-10L Translocations

Shu-Fen Peng, Yao-Pin Lin and Bor-yaw Lin[1]

Institute of Molecular Biology, National Chung Hsing University, Taichung 402, Taiwan, Republic of China

ABSTRACT

Maize B chromosome sequences have been previously cloned by microdissection, and all are proven to be highly repetitive, to be homologous to the normal complement, and to show no similarity to any published gene other than mobile elements. In this study, we isolated sequences from defined B regions. The strategy involved identification and then mapping of AFLP-derived B fragments before cloning. Of 14 B AFLPs, 13 were mapped by 12 B-10L translocations: 3 around the centromeric knob region, 3 in the proximal euchromatic, 1 around the border of proximal euchromatic and distal heterochromatic, and 6 in the distal heterochromatic region of the B long arm. The AFLP fragments were cloned and sequenced. Analogous to the microdissected sequences, all sequences were repetitive, and all but two were highly homologous to the A chromosomes. FISH signals of all but three clones appeared in pachytene B as well as in somatic A and B chromosomes. None of these clones exhibits identity to any published gene. Six clones displayed homology to two centromeric BACs, four to sequences of chromosomes 3, 4, 7, and 10, four to retrotransposons, and three to no sequence deposited in GenBank. Furthermore, flanking regions of two highly B-specific clones were characterized, showing extension of a B-exclusive nature. The possibility of the presence of novel B repeat(s) is discussed.

UNDERSTANDING molecular organization of the B chromosome is a challenge for maize geneticists, as its DNA defies cloning by conventional procedure. The problem stems from its high homology to the A chromosomes. Recently, several approaches have been attempted to overcome this handicap. ALFENITO and BIRCHLER (1993) screened 5000 phages from a B-carrying library and successfully uncovered eight phages, which hybridized strongly with the B DNAs but less so with the DNA without B. Southern hybridization between the phages indicated that they had some sequences in common. A B-specific sequence (pZmBs) was subcloned to hybridize only with the B DNAs but not with the DNA devoid of B. This subclone contained a repeat (CCCTAAA), yielding a positive *in situ* signal on the centromere. This repeat was later demonstrated to be a part of a functional B centromere by KASZÁS and BIRCHLER (1996). STARK *et al.* (1996) isolated B sequences by PCR technology. They compared the RAPD pattern between plants with and without B chromosomes and identified a B-specific RAPD, which showed no hybridization signal with the DNA digest without B but a strong signal with the B DNA

digest. Part of this clone is homologous to the long terminal repeats (LTRs) of retroelement *PREM*-1.

To eliminate interference of the A chromosomes, CHENG and LIN (2003) microdissected B chromosomes out of pachytene slides and amplified with degenerate oligonucleotide-primed PCR to result in 19 new B sequences. Southern analysis and FISH hybridizations illustrated that all are repetitive sequences. Six sequences do not share homology with any published sequence while 10 showed homology either with noncoding regions of clones carrying *adh*1, *bz*1, and *zein* genes or with a *PREM*-2 *gag* gene. Two sequences are related to knob-specific 180-bp repeats, hybridizing with A and B knobs. The last sequence (pBPC51) is B specific; its FISH signal appeared on the B long arm as well as on the centromere. It was placed to the distal heterochromatic region by B-10L translocations and FISH hybridization, spreading over a region of about one-third of the B chromosome. Furthermore, using pBPC51 as probe, they identified a novel B-specific repeat (CL repeat; 1.6 kb) from a λ-library carrying 16 B's (CHENG and LIN 2004).

In this article, B sequences were cloned from 13 B-derived AFLPs located in various B regions defined by 12 B-10L translocations. These AFLPs were mapped, cloned, and sequenced. Of 13 B sequences, all but two shared various degrees of homology with the A chromosomes. The exceptional two sequences were B specific and such B specificity extends to their respective flank-

---

ing regions. Association of the two clones with tandem repeats is discussed.

MATERIALS AND METHODS

Genetic stocks: Two inbreds (W22 and L289) with and without B chromosomes were used to screen B-derived AFLP fragments. L289 carrying 0, 1, 3, and 5 B's (which are referred to as L289 + 0B, L289 + 1B, L289 + 3B, and L289 + 5B, respectively, in this article) and W22 carrying 0, 6, and 16 B's (which are referred to as W22 + 0B, W22 + 6B, and W22 + 16B, respectively, in this article) were utilized to study the dosage analysis of the B-derived AFLPs. Twelve B-10L translocations in the B73/W22 background were used to generate hypoploids. One of their breakpoints is in the long arm of chromosome 10 proximal to the *R* locus. The second breakpoint is located in various regions of the B long arm: four translocations (TB-10L3, TB-10L6, TB-10L7, and TB-10L37) in the proximal euchromatic region and eight (TB-10L1, TB-10L8, TB-10L19, TB-10L20, TB-10L22, TB-10L26, TB-10L32, and TB-10L36) in the distal heterochromatic region (Lin 1978, 1979). These translocations carry the *R-scm* allele, conditioning a uniformly colored aleurone and a deeply colored coleoptile tip, located in the distal 10L.

Synthesis of hypoploids: The procedure for production of hypoploids has been previously published (Lin and Chou 1997). Briefly, hypoploids were produced from the crosses of $10(r)\ 10(r)\ (B73) \times 10(r)\ 10\text{-B B-}10\ (R\text{-}scm)\ \text{B-}10\ (R\text{-}scm)\ (W22)$. After fertilization, two different kernels were produced: one had a colorless embryo associated with a self-colored endosperm and the other had a reverse phenotype. The former bore a hypoploid embryo, which was verified to have 20 chromosomes by chromosome counting in root tips.

Strategy for AFLP mapping: The strategy for mapping AFLPs was according to Lin and Chou (1997) with modifications. Hypoploids produced from B-10L translocations with breakpoints located in various B regions were used for mapping the B-derived AFLPs. The 10-B chromosome of the hypoploid carries the portion of the B distal to the breakpoint. When an AFLP is expressed in a hypoploid, it is mapped in a region distal to the breakpoint, and otherwise it is mapped to a proximal position. On the basis of the presence or absence of an AFLP, 12 hypoploids can be divided into two groups: either proximal or distal to the AFLP. The AFLP is mapped to a region between the most distal breakpoint of the first group and the most proximal breakpoint of the second.

AFLP analysis: AFLP analysis was performed according to the supplier's instructions (system kit I GIBCO BRL, Gaithersburg, MD) on the basis of a description by Vos *et al.* (1995). A total of 250 ng of genomic DNA for each analysis was digested completely with *Eco*RI and *Mse*I (2.5 units each), ligated to adapters (*Eco*RI and *Mse*I adapters; entries 1 and 2, Table 1), and preamplified with primers carrying one selective nucleotide (entries 3 and 4, Table 1). The preamplification PCR program included 20 cycles (30 sec at 94°, 60 sec at 56°, and 60 sec at 72°). The resulting product was diluted 1:50 before using as a template for the second amplification using *Mse*I and end-labeled *Eco*RI primers (both carrying three selective nucleotides at the 3′ end; entries 5–20, Table 1). The second amplification PCR program started with 1 cycle of high annealing temperature (30 sec at 94°, 30 sec at 65°, and 60 sec at 72°) to be followed by 12 cycles of gradually decreasing annealing temperature (0.7° each cycle), and ended with 23 cycles (94° for 30 sec, 56° for 30 sec, and 72° for 60 sec) of low annealing temperature. The final products were loaded into a 6% polyacrylamide denaturing sequencing gel, run at 55 W constant power for 2.5 hr, transferred to 3MM Whatman

TABLE 1

Adapters and primers employed for generation of AFLPs from the B chromosome

Entry	Adapters or primers	Sequences
1	*Eco*RI adapter	5′-CTCGTAGACTGCGTACC-3′
		5′-AATTGGTACGCAGTCTAC-3′
2	*Mse*I adapter	5′-GACGATGAGTCCTGAG-3′
		5′-TACTCAGGACTCAT-3′
3	Pre-*Eco*RI	5′-GACTGCGTACCAATTCA-3′
4	Pre-*Mse*I	5′-GATGAGTCCTGAGTAAC-3′
5	*Eco*RI-AAC	5′-GACTGCGTACCAATTCAAC-3′
6	*Eco*RI-AAG	5′-GACTGCGTACCAATTCAAG-3′
7	*Eco*RI-ACA	5′-GACTGCGTACCAATTCACA-3′
8	*Eco*RI-ACC	5′-GACTGCGTACCAATTCACC-3′
9	*Eco*RI-ACG	5′-GACTGCGTACCAATTCACG-3′
10	*Eco*RI-ACT	5′-GACTGCGTACCAATTCACT-3′
11	*Eco*RI-AGC	5′-GACTGCGTACCAATTCAGC-3′
12	*Eco*RI-AGG	5′-GACTGCGTACCAATTCAGG-3′
13	*Mse*I-CAA	5′-GATGAGTCCTGAGTAACAA-3′
14	*Mse*I-CAC	5′-GATGAGTCCTGAGTAACAC-3′
15	*Mse*I-CAG	5′-GATGAGTCCTGAGTAACAG-3′
16	*Mse*I-CAT	5′-GATGAGTCCTGAGTAACAT-3′
17	*Mse*I-CTA	5′-GATGAGTCCTGAGTAACTA-3′
18	*Mse*I-CTC	5′-GATGAGTCCTGAGTAACTC-3′
19	*Mse*I-CTG	5′-GATGAGTCCTGAGTAACTG-3′
20	*Mse*I-CTT	5′-GATGAGTCCTGAGTAACTT-3′

paper, dried, and exposed to X-ray film (Amersham Pharmacia Biotech Hyperfilm MP) for 16–24 hr.

Recovery of B-derived AFLPs: The polymorphic AFLP fragments were recovered from a gel by the following procedure outlined by Cnops *et al.* (1996). Briefly, the positions of a B-derived AFLP were marked by the use of three needle stabs on a dried gel after placing an unexposed X-ray film underneath in the dark room. Following exposure, the autoradiograph was aligned with the gel. The critical AFLP fragment was identified, excised, and eluted in 400 μl high-salt buffer (20% ethanol, 1 mM LiCl, and 10 mM Tris-HCl pH 7.5) at 65° for 2 hr and precipitated in 95% ethanol at −20° overnight. One-quarter of the resuspended DNA was reamplified with primers of the second amplification PCR. The PCR cycles started with denaturation at 94° for 2 min to be followed by 35 cycles of amplification (30 sec at 94°, 30 sec at 56°, and 1 min at 72°).

Cloning B-derived AFLPs: The pBluescript SK plasmid was digested completely by *Eco*RV to generate blunt ends. Then deoxythymine 5′-triphosphate (dTTP) was added to generate T-vector by *Taq* polymerase. The reaction (5 μg *Eco*RV-digested pBluescript SK plasmid, 1× PCR buffer, 2 mM dTTP, and 5 units Takara Ex *Taq* polymerase) was incubated at 70° for 2 hr. Each product of the B-derived AFLPs was ligated to the T-vector (50 ng T-vector, 100 ng B-derived AFLP fragment, 1× ligation buffer, 400 units New England Biolabs T4 ligase) at 16° overnight, and transformed into host cells (DH5α) according to the protocol of Chung *et al.* (1989) with modifications. The host cells were grown in Luria-Bertani (LB) to the exponential phase (OD600 0.3–0.4), pelleted by centrifugation at $1000 \times g$ for 10 min at 4°, and resuspended in one-tenth of their original volume of ice-cold transformation and storage solution [TSS: LB broth with 10% (w/v) PEG8000, 5% (v/v) DMSO, and 50 mM MgCl2]. An aliquot was transferred to

TABLE 2

AFLP-derived B sequences and accession numbers in GenBank

Clone no.	Accession no.
E32M47$_1$	CL603061
E32M47$_2$	CL603055
E32M59	CL603066
E35M59$_2$	CL603056
E35M61	CL603057
E36M62$_1$	CL603065
E36M62$_2$	CL603063
E37M49	CL603058
E38M49	CL603059
E38M50	CL603060
E40M49	CL603064
E41M50$_1$	CL603062
E41M50$_2$	CL603067
pAFB1	CL603068
pAFB1E	CL603069
pAFB2	CL603070

a cold microcentrifuge tube, mixed with the ligated DNA, and incubated for 30 min at 4°. Next, 0.9 ml TSS with 20 mM glucose was added to the mixture, and the cells were grown at 37° with shaking (150 rpm) for 1 hr to allow expression of the antibiotic-resistance gene. Finally, transformants were selected by plating the cells onto solid LB agar plates containing ampicillin (50 μg/ml), X-gal (50 μg/ml), and IPTG (50 μg/ml) at 37° overnight.

Southern analysis: Protocols of genomic DNA isolation, DNA restriction digestion and blotting onto filters, probe preparation, prehybridization, hybridization, washing, and exposure have been published previously (LIN *et al.* 1997).

Sequence analysis: Sequence comparison was performed using BLAST software of the National Center for Biotechnology Information (NCBI) website. Sixteen were registered in the genome survey sequences database (dbGSS) of GenBank. Their accession numbers are listed in Table 2.

Preparation of pachytene chromosomes for *in situ* hybridization: Pachytene chromosomes were prepared by following the protocol of CHEN *et al.* (1998) with modifications. Microsporocytes (L289 + 2B) were collected, fixed in ethanol-glacial acetic acid (3:1), and stored at −20°. A single anther of desirable pachytene stage was placed in a drop of enzyme buffer (4 mM citric acid, 6 mM sodium citrate, pH 4.8) on a slide for 10 min, treated with enzyme mixture [2% (w/v) Onozuka R10 cellulase (Yakult honsha), 1% (w/v) macerozyme R10 (Yakult honsha), and 1% cytohelicase (Sigma, St. Louis)] in enzyme buffer at room temperature for 3 hr, and gently squeezed out microsporocytes in a drop of 45% acetic acid by a needle. After discarding the anther walls, microsporocytes were covered with a coverslip, which was then removed with a razor blade after freezing in liquid nitrogen.

Preparation of metaphase spreads from root tips: Root tips (W23 + 2B) were cut, pretreated in saturated 1-bromonaphtalene containing 0.25% (v/v) DMSO at room temperature for 4 hr, fixed in 3:1 ethanol-acetic acid, treated in enzyme buffer (4 mM citric acid, 6 mM sodium citrate, pH 4.8) for 10 min, incubated in the above-mentioned enzyme mixture at 37° for 4 hr, softened in 45% acetic acid for 10 min, and resuspended in 50 μl 1:1 ethanol-acetic acid. An aliquot was placed onto acid-cleaned slides, which were air dried and stored in desiccators.

Fluorescence *in situ* hybridization: Probe preparation, hybridization, and signal detection have been previously described by CHENG and LIN (2003, 2004). The signal location data were collected from observation of 5–10 B chromosomes on one to two slides.

Construction of genomic library: Construction of the genomic library has been previously described by CHENG and LIN (2004). Clones p3259 and p4049 were used for screening the genomic library in this study.

RESULTS

Isolation of B-derived AFLPs: A total of 64 primer pairs were used to screen W22 and L289 with and without B for B polymorphism (Table 1). Two inbreds were included as negative controls. Ten primer combinations generated 14 B fragments, which were designated according to the system formulated by VUYLSTEKE *et al.* (1999), including two primer codes followed by their fragment size as shown in Table 3. Four of the primer pairs yielded two B fragments (Figure 1, A and B, D and E, G and H, M and N), while the other six primer pairs yielded a single fragment each (Figure 1, C, F, I, J, K, and L). Expression of the B fragments in W22 and L289 was consistent between W22 and L289, except for E35M59$_2$ (Figure 1E), which appeared in DNAs carrying the B chromosomes (lanes 2 and 4) but also manifested faintly in L289—not W22—DNAs (lane 3). The fragment sizes range from 86 bp for E36M62$_2$ to 268 bp for E35M61 (Table 3). Two types of B fragments were observed: the B fragments that occurred exclusively in the B-carrying DNAs (W22 + 4B and L289 + 3B) and those appearing in DNAs with and without B with the signal in the former very intense but in the latter hardly visible. The first B-fragment type includes 10 fragments (Figure 1, A–N, except C, F, I, and J) and the second type four (Figure 1, C, F, I, and J). An example of the first type is E32M47$_1$ (Figure 1A), which appears only in W22 + 4B (lane 2) and L289 + 3B (lane 4), and an example of the second type is E37M49 (Figure 1I) with signal in DNAs with and without the B chromosome. For convenience of discussion, all fragments, whether B specific or not, were termed AFLPs in this article.

B-dosage effect of AFLPs: The fact that these AFLPs originated from the B chromosome is substantiated by their response to the B number. A B fragment so derived would be expected to augment its signal intensity in parallel with the increase in the B number. This was indeed found to be the case. All 14 AFLPs enhanced their signal in a B-dosage-dependent manner (Figure 2 and Table 3). An example is shown in Figure 2A where the B-specific signal (E32M47$_1$) was not detectable in the L289 track (lane 1), but it was observed in the tracks of L289 + 1B, L289 + 3B, and L289 + 5B (lanes 2–4) with its intensity gradually increasing as the B number rose from 1 to 5. Another fragment (E37M49) is not B specific (Figure 2I), but its signal in the B tracks enhances in a similar pattern.

<div align="center">

TABLE 3

Characteristics of 14 B chromosome AFLPs

</div>

Designation		Primer pairs	Molecular size (bp)[d]	B-dosage effect
Standard[a]	Short form[b]			
$E32M47_{133}$	$E32M47_1$	*Eco*RI-AAC/*Mse*I-CAA[c]	133	+
$E32M47_{118}$	$E32M47_2$	*Eco*RI-AAC/*Mse*I-CAA[c]	118	+
$E32M59_{110}$	E32M59	*Eco*RI-AAC/*Mse*I-CTA	110	+
$E35M59_{140}$	$E35M59_1$	*Eco*RI-ACA/*Mse*I-CTA[c]	140	+
$E35M59_{128}$	$E35M59_2$	*Eco*RI-ACA/*Mse*I-CTA[c]	128	+
$E35M61_{268}$	E35M61	*Eco*RI-ACA/*Mse*I-CTG	268	+
$E36M62_{209}$	$E36M62_1$	*Eco*RI-ACC/*Mse*I-CTT[c]	209	+
$E36M62_{86}$	$E36M62_2$	*Eco*RI-ACC/*Mse*I-CTT[c]	86	+
$E37M49_{114}$	E37M49	*Eco*RI-ACG/*Mse*I-CAG	114	+
$E38M49_{229}$	E38M49	*Eco*RI-ACT/*Mse*I-CAG	229	+
$E38M50_{145}$	E38M50	*Eco*RI-ACT/*Mse*I-CAT	145	+
$E40M49_{203}$	E40M49	*Eco*RI-AGC/*Mse*I-CAG	203	+
$E41M50_{207}$	$E41M50_1$	*Eco*RI-AGG/*Mse*I-CAT[c]	207	+
$E41M50_{179}$	$E41M50_2$	*Eco*RI-AGG/*Mse*I-CAT[c]	179	+

[a] Designation according to Vuylsteke *et al.* (1999).

[b] Designation used in this article (subscript 1, large AFLP fragment; subscript 2, small AFLP fragment).

[c] Two AFLPs generated from a single primer pair.

[d] Molecular weight in the gel estimated by Kodak Digital Science 1D.

Physical mapping of AFLPs by hypoploids of B-10L translocations: The structure of the B chromosome (Figure 3) is highly heterochromatic (McClintock 1933; Randolph 1941). At the pachytene stage it has a minute short arm, a centromeric knob (CK; including the centromere and proximal heterochromatic region), and a long arm composed of—from proximal to distal end—a proximal euchromatic region (PE), a distal heterochromatic region (DH), and a distal euchromatic tip (DE). DH consists of four distinctive blocks: DH1, DH2, DH3, and DH4 (Figure 3; Beckett 1991; Cheng and Lin 2003).

AFLPs were mapped by 12 B-10L translocations whose breakpoints dispersed from PE to DH of the B long arm. Of these translocations, TB-10L3, TB-10L6, TB-10L7,

and TB-10L37 break in PE; TB-10L19 in DH1; TB-10L1, TB-10L8, and TB-10L22 in DH1–DH2 (exact location unknown); TB-10L26 and TB-10L32 in DH2 closed to the DH2/DH3 junction; and TB-10L20 and TB-10L36 in DH3 near the DH3/DH4 junction (Beckett 1991; Cheng and Lin 2003). The mapping strategy (see MATERIALS AND METHODS) utilized hypoploids, which contain the 10-B, the critical element, carrying the distal portion of the B long arm, but not the B-10 associated with the proximal B portion. If an AFLP is produced from a hypoploid of a particular B-10L translocation, its locus is distal to the breakpoint of the translocation; that is, it is located on the 10-B. Otherwise, it is proximal to the breakpoint; it is on the B-10.
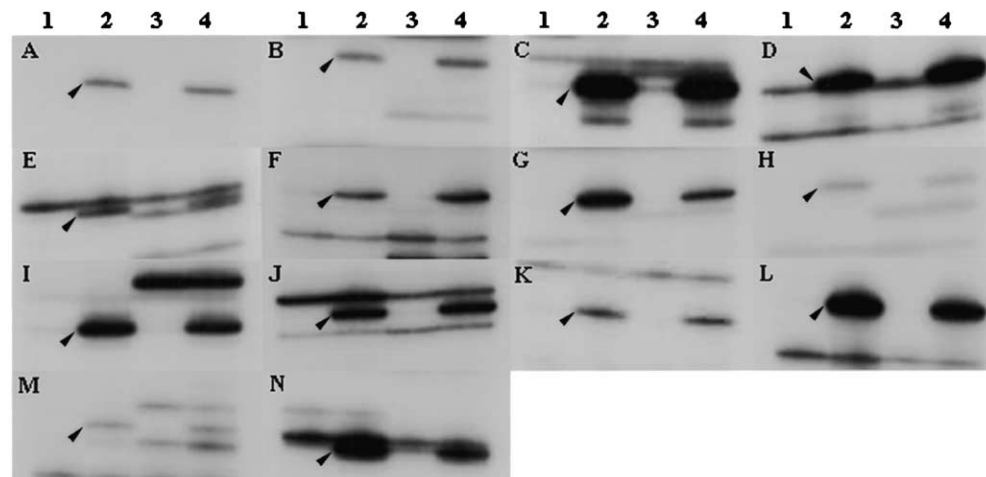

Figure 1.—Fourteen B-derived AFLPs generated from 10 primer combinations. (A) $E32M47_1$. (B) $E32M47_2$. (C) E32M59. (D) $E35M59_1$. (E) $E35M59_2$. (F) E35M61. (G) $E36M62_1$. (H) $E36M62_2$. (I) E37M49. (J) E38M49. (K) E38M50. (L) E40M49. (M) $E41M50_1$. (N) $E41M50_2$. Lane 1, W22; lane 2, W22 + 4B; lane 3, L289; lane 4, L289 + 3B. Arrowheads indicate B fragments. Four primer pairs yielded two B fragments and six generated one. Two AFLPs generated by a single primer pair were distinguished by subscripts 1 (large fragment) and 2 (small fragment), respectively.
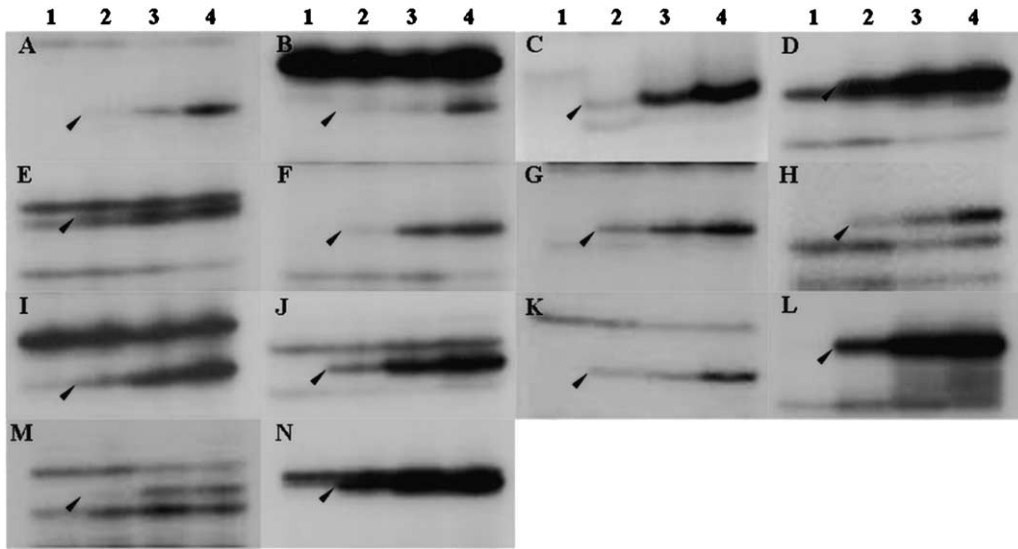
FIGURE 2.—Dependence of AFLP intensity on the B dosage. Origin of 14 AFLPs were confirmed by their response to B dosage. Intensity of some non-B-specific bands in the figure (C, E, F, J, K, H, and M) is likewise variable but not in the B-dosage-dependent manner, probably due to residual local sequence variation at the priming sites between different lines. (A) $E32M47_1$. (B) $E32M47_2$. (C) E32M59. (D) $E35M59_1$. (E) $E35M59_2$. (F) E35M61. (G) $E36M62_1$. (H) $E36M62_2$. (I) E37M49. (J) E38M49. (K) E38M50. (L) E40M49. (M) $E41M50_1$. (N) $E41M50_2$. Lane 1, L289; lane 2, L289 + 1B; lane 3, L289 + 3B; lane 4, L289 + 5B. Arrowheads indicate B fragments.

Of the 14 AFLPs mapped with this strategy, 13 were successfully placed on the B chromosome and one was not. The hypoploid mapping divided the 13 AFLPs into two groups. The first group, located in DH, was amplified from the hypoploids of four translocations (TB-10L3, TB-10L6, TB-10L7, and TB-10L37) whose breakpoints are proximal to DH, indicating its locus in DH (Figures 3 and 4A). By a process of elimination, the second group is located in PE, and its location is substantiated by analyses of eight other B-10L translocations (TB-10L1, TB-10L8, TB-10L19, TB-10L20, TB-10L22, TB-10L26, TB-10L32, and TB-10L36), all of which break in DH; its 10-B chromosome is deficient of PE. As would be expected, the hypoploids expressed no signal of this group (Figure 4A).

The first group was further divided into five subgroups by eight translocations with breakpoints in DH (Figures

3 and 4A). The hypoploid of TB-10L36 amplified only subgroup 1 ($E41M50_2$ and E32M59; see below); that of TB-10L20 subgroup 2 ($E36M62_1$; see below) in addition to subgroup 1; that of TB-10L26 and TB-10L32 subgroup 3 (E40M49) plus two previous groups; that of TB-10L1 and TB-10L19 subgroup 4 ($E36M62_2$) plus three previous groups; and that of TB-10L8 and TB-10L22 subgroup 5 ($E41M50_1$) in addition to the four preceding groups. Of these signals, one (E32M59) amplified from hypoploids of TB-10L20 and TB-10L36 and the other ($E36M62_1$) from the hypoploid of TB-10L20 was less intense than that of the same signals amplified from other hypoploids. Such signal reduction—which is not due to insufficient DNA loading as it is evident in comparison with control signal (Figure 4B)—represents multiple signal loci spreading on both sides of the two breakpoints. In short, the map order of the first group relative to translo-
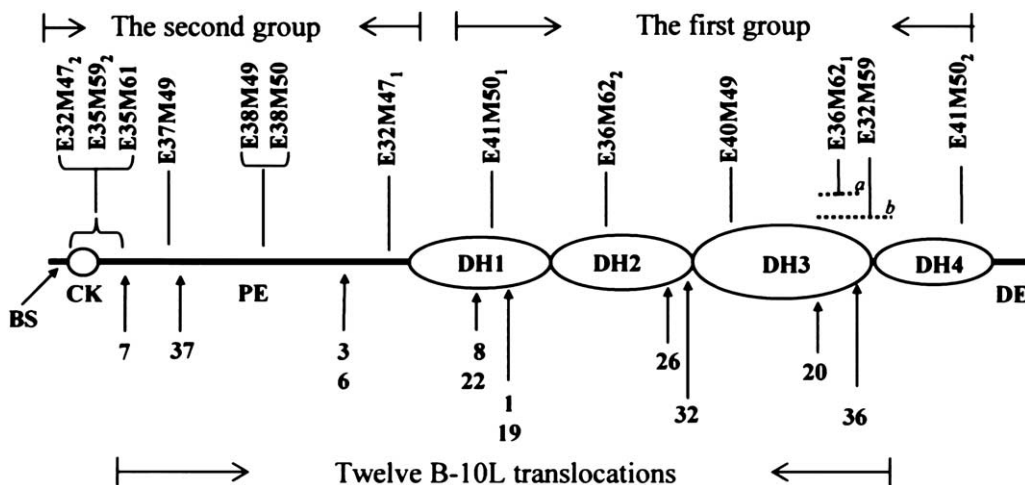

FIGURE 3.—Map position of 13 AFLPs in relation to the breakpoints of 12 B-10L translocations. BS, short arm of the B chromosome; CK, centromeric knob, including centromere and proximal heterochromatic region; PE, proximal euchromatic region; DH1–4, distal heterochromatic region; DE, distal euchromatic region. *a* and *b* indicate the probable distributions of $E36M62_1$ and E32M59, respectively.
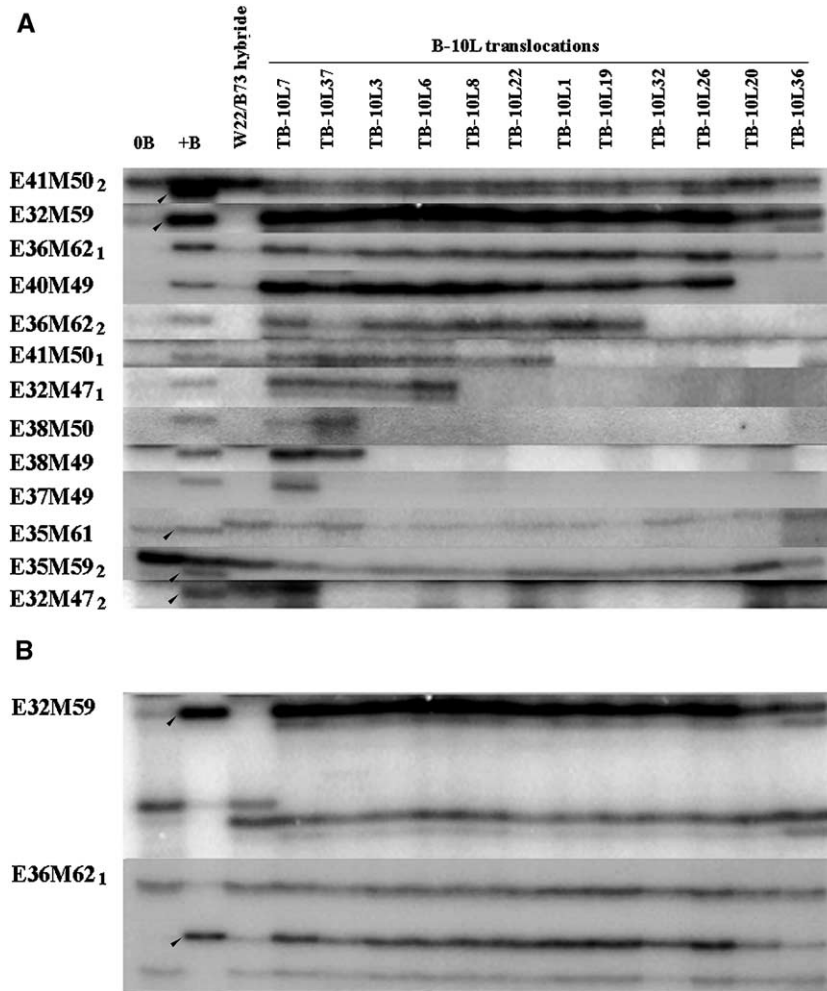
FIGURE 4.—Mapping 13 AFLPs by hypoploids of 12 B-10L translocations. (A) The AFLP location on the B chromosome is determined by presence or absence of B signals in the hypoploid DNAs. The +B lanes were loaded with either W22 + 1B (most clones) or W22 + 4B (E41M50$_2$, E35M59$_2$, and E32M47$_2$). (B) Reduction of signals associated with E32M59 and E36M62$_1$ was compared with control. The B fragments are shown by arrowheads.

cation breakpoints is as follows (Figure 3): telomere—subgroup 1—TB-10L36—subgroup 2—TB-10L20—subgroup 3—TB-10L26/TB-10L32—subgroup 4—TB-10L1/TB-10L19—subgroup 5—TB-10L8/TB-10L22—PE. In terms of the pachytene structure, the approximate location of subgroup 1 is in the junction between DH4 and DE (DH4/DE), subgroups 2 and 3 in DH3, subgroup 4 in the junction between DH1 and DH2 (DH1/DH2), and subgroup 5 in DH1.

The second group is likewise divided into four subgroups by the four translocations mentioned above, which break in various regions of PE (Figures 3 and 4A). Subgroup 1 (E32M47$_1$) was amplified from the hypoploids of all four translocations, subgroup 2 (E38M49 and E38M50) from those of TB-10L7 and TB-10L37, and subgroup 3 (E37M49) from those of TB-10L7. Subgroup 4 (E32M47$_2$, E35M59$_2$, and E35M61) was not produced from any of the four hypoploids but the B chromosome. These data place subgroup 1 to the most distal position, subgroup 4 to the most proximal one, and the remaining two subgroups in between (Figure 3). The map order in relation to breakpoints is DH—subgroup 1—TB-10L3/TB-10L6—subgroup 2—TB-10L37—subgroup 3—TB-10L7—subgroup 4—centromere. The lo-

cation of subgroup 4 is difficult to pinpoint. It is located in the PE proximal to TB-10L7, which includes the short arm, the centromeric knob, and the proximal portion of PE (LIN 1978). The likelihood of its location in the short arm can be excluded, since these signals were not amplified from the hypoploid of TB-10L18, the 10-B of which carries the B short arm (LIN 1979; data not shown).

Cloning of AFLPs: Sequences cloned from the gel of an AFLP may be of various sorts, and the authentic sequence is distinguished by its length compared to the original AFLP. Furthermore, since an AFLP is single stranded and the cloned sequence is double stranded, the latter needs to be converted into single-strand conformation before its length is measured. To achieve this, the procedure of XU et al. (2001) was adopted in this study. An AFLP was retrieved from the dried gel, amplified with the original AFLP primers (see MATERIALS AND METHODS), and finally cloned into the pBluescript vector. Three to six colonies from each AFLP were reamplified using the same primers. The double-strand products along with those of the original AFLP were denatured and analyzed in denaturing polyacrylamide gel to compare mobility of these products with the AFLP.
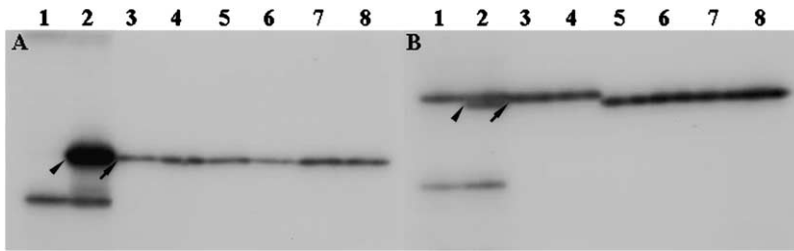
FIGURE 5.—Size variation of clones from an AFLP resolved in denaturing polyacrylamide gel. (A) Six clones (lanes 3–8) from E40M49 comigrate with the original AFLP (lane 2). (B) Six others (lanes 3–8) from E35M59$_2$ have two different sizes, four (lanes 5–8) of which are comparable to the original AFLP (lane 2) and two others (lanes 3–4) of which are larger. The arrowhead shows the original AFLP, and the arrow indicates its derived clones. Lane 1, W22; lane 2, W22 + 4B; lanes 3–8, six clones derived from an AFLP.

Of the 14 AFLPs, 1 (unmapped) was not cloned, 7 gave rise to clones the same size as their original AFLP, and 6 others carried a fragment of the expected size as well as a second fragment with a size slightly different from the original AFLP. The clone whose amplified products comigrated with the original AFLP was selected for further analysis. Figure 5A depicts six clones from E40M49, all (lanes 3–8) of which had the same mobility as the original AFLP (lane 2), and Figure 5B shows six others from E35M59$_2$, four (lanes 5–8) of which had the same mobility as the original AFLP (lane 2) and two others of which did not (lanes 3–4).

Characterization of AFLP sequences: To further prove the B origin of the cloned sequences, the *Eco*RI digests of genomic DNAs carrying 0, 6, and 16 B's (W22 + 0B, W22 + 6B, and W22 + 16B) were hybridized with each AFLP-derived sequence as probe. If a sequence originates from the B chromosome, its intensity of the hybridization signal should be proportional to the number of B chromosomes present in the genome (dosage effect). Of the 13 cloned sequences analyzed as such, 5 had signal intensities that were proportional to the B number (Figure 6, B, D, J, K, and L) while 5 others had markedly fewer signals of this nature (Figure 6, C, E, G, H, and M), and the last 3 had none (Figure 6, A, F, and I). Hence, the first 10 sequences were evidently derived from the B chromosome, and the origin of the last 3 sequences could not be determined on the basis of the results of this study.

Table 4 summarizes four hybridization types in *Eco*RI digests. All displayed multiple copy, and all but one (type IV) carried all or some signals that were B-dosage dependent. Type I, including two clones (Figure 6, J and L), had discrete and smeared signals—with all discrete signals being B specific—in the W22 + 6B and W22 + 16B DNAs. But their signals in the DNA without B's (W22 + 0B) are dependent on the exposure condition, that is, no signal under regular exposure but weakly smeared after a prolonged exposure (they were referred to as B-specific clones in this report). Type II signal was similar to type I but with only a few discrete signals being B specific. (Figure 6, B, D, and K). Type III was associated with smeared background in addition to discrete bands, some of which showed B-dosage effect (Figure 6, C, E, G, H, and M). Type IV was heavily smeared and not B-number dependent (Figure 6, A, F, and I).

These patterns are independent of the B chromosome regions where these clones are located (Figure 6 and Table 4). Three clones (p3247$_2$, p3559$_2$, and p3561; Figure 6, A–C, respectively) situated in CK and proximal PE, three clones (p3749, p3849, and p3850; Figure 6, D–F, respectively) in PE, one clone (p3247$_1$; Figure 6G) in the PE/DH1 junction region, and the last six clones (p4150$_1$, p3662$_2$, p4049, p3662$_1$, p3259, and p4150$_2$; Figure 6, H–M, respectively) located in the DH region. The hybridization patterns of the first two and the last region are similar, consisting of three types (types II, III, and IV; Table 4), with the exception of DH where two clones (p4049 and p3259) were B specific and B-number dependent (Figure 6, J and L). In short, from the centromere to the most distal end of the B long arm, hybridization patterns of the 13 B sequences from defined regions are randomly distributed (Figure 6).

In addition to *Eco*RI, three other enzymes, *Eco*RV, *Hin*fI (a 5-bp cutter), and *Mse*I (a 4-bp cutter), were likewise used for Southern analysis of these B sequences (data not shown). Treatment of *Eco*RV resulted in a hybridization pattern similar to that of *Eco*RI. Digestions of *Hin*fI and *Mse*I did not change the basic patterns of type I and type II described above, but shifted types III and IV to a pattern similar to type II but retaining their original characteristic response to the B number; that is, only a few signals of type III exhibited a B-dosage effect but none of the type IV did (data not shown).

The location of the 13 clones was further confirmed by FISH analysis on the pachytene B chromosme. As shown in Figure 7 and Table 5, when each was used as probe, all but 3 clones expressed signals over all regions of the B long arm, including euchromatic (PE and DE) and heterochromatic (CK and DH) regions (Table 5). The signal intensity of some (such as p3247$_2$; Figure 7A and entry 1, Table 5) was weak, and that of others (such as p3850; Figure 7B and entry 6, Table 5) was intense. Two of the exceptional clones (p3259 and p4049) displayed faint signals mostly in DH3—with a few in DH2/DH4—regions (p3259; Figure 7C and entry 12, Table 5) and in the DH1/DH3 junction (p4049; Figure 7D and entry 10, Table 5), respectively. The last clone (p3749; entry 4, Table 5) gave no signal, and, as mentioned above, it is also the one that weakly hybridized to genomic DNA (Figure 6D).

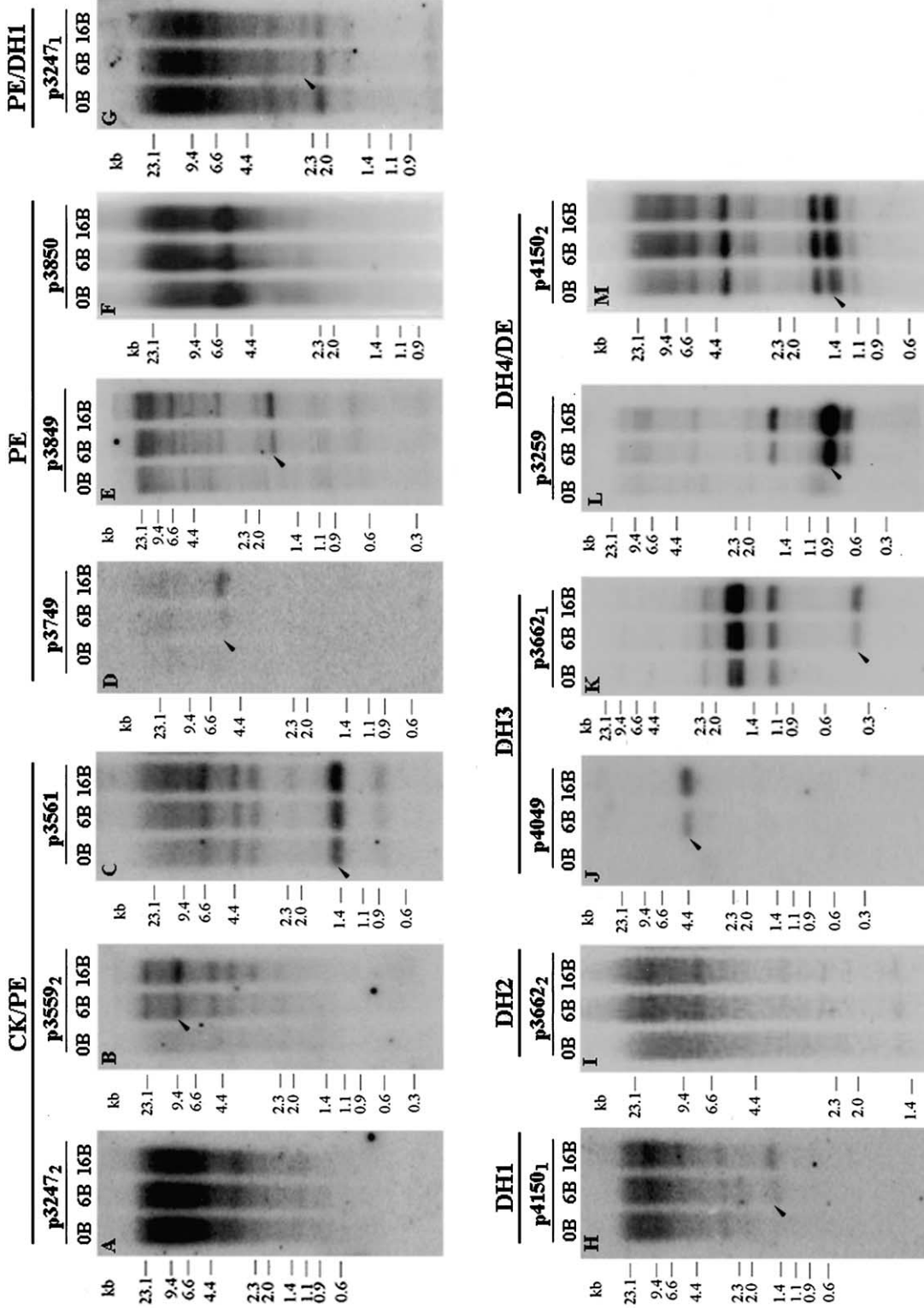To understand distributions of these clones in the A

FIGURE 6.—Genomic organization of AFLPs located in various B regions. Genomic DNA with 0, 6, and 16 B's were digested with *Eco*RI and probed by the following B sequences: p3247₂ (A), p3559₂ (B), p3561 (C), p3749 (D), p3849 (E), p3850 (F), p3247₁ (G), p3662₂ (I), p4049 (J), p4150₁ (H), p3662₂ (I), p4049 (J), p4150₁ (K), p3259 (L), and p4150₂ (M). Arrowheads indicate the signals as either B specific or B-dosage dependent. CK/PE, region close to the junction between CK and PE; PE, proximal euchromatic region; PE/DH1, region close to the junction between PE and DH1; DH1–4, distal heterochromatic region; DH4/DE, region close to the junction between DH4 and DE.

TABLE 4

Southern characteristics of 13 B clones derived from AFLPs

| | Designation | | | | |
| | Isolated clones | Original AFLPs | Dosage effect[a] | B specificity[b] | Location[c] |
Type					
I	p3259	E32M59	+	+	DH4/DE
	p4049	E40M49	+	+	DH3
II	$p3559_2$	$E35M59_2$	+	+	CK/PE
	$p3662_1$	$E36M62_1$	+	+	DH3
	p3749	E37M49	+	+	PE
III	p3849	E38M49	±	+	PE
	$p3247_1$	$E32M47_1$	±	+	PE/DH1
	p3561	E35M61	±	−	CK/PE
	$p4150_1$	$E41M50_1$	±	+	DH1
	$p4150_2$	$E41M50_2$	±	−	DH4/DE
IV	$p3247_2$	$E32M47_2$	−	−	CK/PE
	$p3662_2$	$E36M62_2$	−	−	DH2
	p3850	E38M50	−	−	PE

[a] +, responsive to the B numbers; ±, some signals responsive to the B numbers; −, no response to the B number.

[b] +, presence of signals only in the W22 + 6B and W22 + 16B DNAs; −, presence of signals in the W22 + 0B, W22 + 6B, and W22 + 16B DNAs.

[c] AFLP location on the B chromosome. CK, centromeric knob including centromere and proximal heterochromatic region; PE, proximal euchromatic region; DH, distal heterochromatic region; DE, distal euchromatic region; CK/PE, region close to the junction between CK and PE; PE/DH1, region close to the junction between PE and DH1; DH4/DE, region close to the junction between DH4 and DE.

chromosomes, the same probes were used to hybridize with mitotic metaphases of root-tip spreads carrying two B chromosomes (W23 + 2B). Three clones (p3259, p3749, and p4049) did not show a signal in either A's or B's (data not shown), and the remaining clones displayed FISH signals in both A's and B's. Two representative clones were shown in Figure 7, where $p3247_2$ revealed weak signal in the B chromosome and scattered signals in A's (Figure 7G), while p3850 yielded more intense signals in both A's and B's (Figure 7H).

Thirteen B sequences were sequenced and analyzed by BLAST 2 sequences (Tatusova and Madden 1999). The average length of the sequences is 140 bp (65–249 bp; Table 6), and the average A + T bases is 61%. All sequences showed no homology to each other. No repeat longer than 14 bp was observed. Of 13 sequences analyzed by a tandem repeat finder (Benson 1999), no tandem repeat was apparent in 7 sequences and short tandem repeats of 2–13 bp were apparent in 6 others (data not shown). Only seven clones carried open reading frames (ORFs) with 35–73 codons (Table 6). Whether or not these ORFs are valid cannot be determined until the regions flanking these sequences are available.

Every B sequence was used as a query in GenBank search for homologous sequences (Table 6). Three sequences ($p3559_2$, p3749, and p4049; entries 2, 4, and 10,

respectively) did not display homology to any published maize sequence, and 10 others had similarity to maize clones with no known functions. Clones p3561 (entry 3; nt 22–248), $p3662_2$ (entry 9; nt 12–58), and p3850 (entry 6; nt 1–103) had identity to various regions of ZM15C05 (nt 949–723, 91% identity; nt 81788–81834, 87% identity; nt 75060–74959, 98% identity, respectively; GenBank accession no. AC116033); $p3662_1$ (entry 11; nt 7–186) to ZM16H10 (nt 12573–12753, 90% identity; GenBank accession no. AC116034); $p4150_1$ (entry 8; nt 1–180) to BAC 163K15 (nt 17246–17429, 90% identity; GenBank accession no. AF466931); and $p3247_1$ (entry 7; nt 34–60) to PCO103020 mRNA (nt 349–375, 96% identity; GenBank accession no. AY107006).

Three clones had homology to the noncoding regions flanking published genes. The B-specific clone p3259 (entry 12; nt 11–83) showed homology to an upstream region of the rust-resistant rp3-1 gene (nt 68437–68509, 89% identity; GenBank accession no. AY574035). Most of p3849 (entry 5; nt 68–212) shared sequence analogy to the region between azs22-15 and azs22-17 of the 22-kD zein clone (nt 116705–116849, 98% identity; GenBank accession no. AF090447), and $p3247_2$ (entry 1; nt 1-87) to the 19 kD of zein gene family (nt 143633–143547, 93% identity; GenBank accession no. AF546188).

Finally, four clones shared sequences with retroelements. Clone $p4150_2$ (entry 13; nt 42–151) carried sequence comparable to the pol gene of Xilon2 of the B73 9S bz genomic clone (nt 5888–5997; 81% identity; GenBank accession no. AF448416), and $p3662_2$ (entry 9; nt 12–58) to the gag gene of Zeon1 of A188 (nt 1701–1747, 85% identity; GenBank accession no. U11059). The majority of sequences of p3850 (entry 6; nt 5–112) were in common with Prem-1 of W22 (nt 628–521; 93% identity; GenBank accession no. ZMU03680) in addition to ZM15C05—the same sequences mentioned above. Clone $p3247_1$ (entry 7; nt 34–60) displayed homology to LTR of Xilon2 of B73 9S bz genomic clone (nt 45677–45703; 96% identity, GenBank accession no. AF448416) plus the same region of PCO103020 mRNA sequences described above.

Characterization of sequences contiguous to the two B-specific clones: Being relatively B specific and repetitive, clones p3259 and p4049 are interesting, as they may be exploited for isolation of large B fragments from B regions different from those previously reported by Cheng and Lin (2004). Unfortunately, other than those hypoploid analyses mentioned previously, the location of these two clones on the B chromosome cannot be confirmed by FISH analysis, since the signal was either very faint or not detectable by the in situ protocol of this laboratory. To overcome this drawback as well as to attempt to search for sequence with better B specificity, fragments flanking the two clones were characterized.

To this end, each clone was used to screen 2000 λ-phages from a 16 B-carrying library to result in five positive phages each, one of which was transferred to
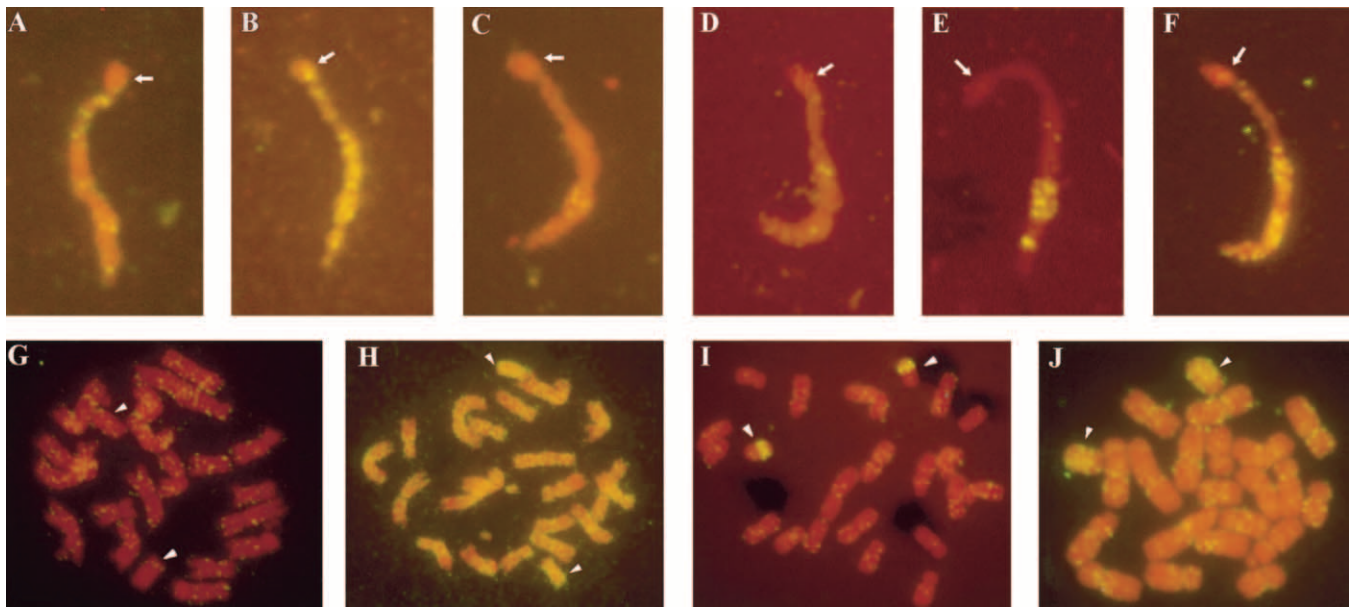
FIGURE 7.—FISH analysis of B clones in pachytene B chromosomes and root-tip spreads. The chromosome stain is red and the B signal is yellowish. Arrows indicate the centromeric knob and arrowheads indicate the B chromosomes. Pachytene signals of $p3247_2$ (A) appear unevenly in the entire B, p3850 (B) appears intensely in all the B long arm, p3259 (C) is very faint in DH3, p4049 (D) is very weak in DH1/DH3, pAFB1E (E) in DH3/DH4, and pAFB2 (F) in the entire B chromosome. The root-tip FISH of $p3247_2$ (G), p3850 (H), pAFB1E (I), and pAFB2 (J) covered all A's and B's with the exception of pAFB1E, which possesses a high degree of B specificity.

pBluescript SK vector. The resulting p3259-carrying *Hinc*II/*Bgl*II fragment (pAFB1, Figure 8A), the *Eco*RI fragment flanking the 5′ side of p3259 (pAFB1E, Figure 8A), and the p4049-carrying *Eco*RV/*Xho*I fragment (pAFB2, Figure 8B) were used to probe genomic DNA

TABLE 5

Location of FISH signal of 16 B sequences in the pachytene B chromosome

Entry	B clones	Position[a]
1	$p3247_2$	CK, PE, DH1, DH2, DH3, DH4, DE
2	$p3559_2$	PE, DH1, DH2, DH3, DH4
3	p3561	CK, PE, DH1, DH2, DH3, DH4
4	p3749	No detectable signal
5	p3849	CK, PE, DH1, DH2, DH3, DH4, DE
6	p3850	CK, PE, DH1, DH2, DH3, DH4, DE
7	$p3247_1$	CK, PE, DH1, DH2, DH3, DH4, DE
8	$p4150_1$	PE, DH1, DH2, DH3, DH4, DE
9	$p3662_2$	CK, PE, DH1, DH2, DH3, DH4
10	p4049	DH1, DH2, DH3
11	$p3662_1$	CK, PE, DH1, DH2, DH3, DH4
12	p3259	DH2, DH3, DH4
13	$p4150_2$	CK, PE, DH1, DH2, DH3, DH4, DE
14	pAFB1	DH1, DH2, DH3, DH4
15	pAFB1E	DH1, DH2, DH3, DH4
16	pAFB2	CK, PE, DH1, DH2, DH3, DH4

[a] B location as designated in Figure 3: BS, short arm; CK, centromeric knob including centromere and proximal euchromatic region; PE, proximal euchromatic region; DH, distal heterochromatic region; DE, distal euchromatic tip.

with and without B chromosomes. pAFB1 and pAFB1E (Figure 8, C2 and D2) gave patterns closely resembling the pattern of p3259 (Figure 6L) in the W22 + 6B and W22 + 16B DNAs carrying a prominent 0.8-kb signal in addition to three and two minor signals, respectively. A less intense, 0.8-kb signal was also present in the W22 + 0B DNA. On other hand, similar to p4049 (Figure 6J), pAFB2 expressed the 4.4-kb signal and an additional 6.5-kb signal in the W22 + 6B and W22 + 16B DNAs, but only very lightly smeared signal in the W22 + 0B DNA (Figure 8E2).

Contrary to Southern hybridization, FISH analysis of flanking clones was dissimilar to that of p3259 and p4049. For p3259, only a very light signal was detected in the pachytene chromosome (Figure 7C) and no signal was detected in root-tip spreads (data not shown). Yet, its flanking clone (pAFB1E, Figure 7E) showed clear pachytene FISH in DH3/DH4 regions, and a highly conspicuous FISH in the B's but only a few discernible weak signals in A's of root-tip spreads (Figure 7I). Similar results were seen in pAFB1 except for the presence of more intense A signals in root-tip cells (data not shown). The pachytene FISH of p4049 and pAFB2 were likewise different: the former had very weak FISH in DH1/DH3 (Figure 7D) but the latter displayed strong FISH over the entire B (Figure 7F). In somatic cells, p4049 showed no visible signal in either A's or B's (data not shown) but pAFB2 manifested dense signals in B's and scattered signals in A's (Figure 7J).

Sequence analysis of pAFB1, pAFB1E, and pAFB2 is

TABLE 6

Sequence characteristics of 13 AFLP-derived and three flanking sequences

Entry	B clones	Size (bp)	A/T (%)	Sequences in GenBank	X^a	Y^b	Z^c
					Nucleotide comparison		
1	p3247$_2$	92	63	*Zea. mays* contiguous sequence of the 19-kD *zein* gene family	1–87	93	—
2	p3559$_2$	99	75	None	—	—	—
3	p3561	249	58	*Z. mays* genomic clone ZM15C05 sequence	22–248	91	73
4	p3749	91	58	None	—	—	—
5	p3849	212	56	*Z. mays* flanking sequences of a 22-kD α *zein* gene cluster	68–212	98	44
6	p3850	116	72	*Z. mays* genomic clone ZM15C05 sequence	1–103	98	35
				Z. mays W22 *Prem*-1 retroelement	5–112	93	
7	p3247$_1$	105	61	*Z. mays* PCO103020 mRNA sequence	34–60	96	—
				Z. mays B73 chromosome 9S *bz* genomic clone (LTR of *Xilon*2)	34–60	96	
8	p4150$_1$	183	64	*Z. mays* clone BAC 163K15	1–180	90	54
9	p3662$_2$	65	54	*Z. mays* genomic clone ZM15C05 sequence	12–58	87	—
				Z. mays A188 *gag* gene of *Zeon*1 retrotransposon	12–58	85	
10	p4049	180	64	None	—	—	59
11	p3662$_1$	186	64	*Z. mays* genomic clone ZM16H10 sequence	7–186	90	35
12	p3259	83	65	Upstream region of *Z. mays* rust resistance protein *rp*3-1 gene	11–83	89	—
13	p4150$_2$	154	49	*Z. mays* B73 chromosome 9S *bz* genomic clone (*pol* gene of *Xilon*2 retrotransposon)	42–151	81	37
14	pAFB1	543	55	Upstream region of *Z. mays* rust resistance protein *rp*3-1 gene	1–500	89	61
15	pAFB1E	727	54	Upstream region of *Z. mays* rust resistance protein *rp*3-1 gene	5–727	91	88
16	pAFB2	1003	59	*Z. mays* genomic clone ZM15C05 sequence (LTR of *Zeon*1a)	574–739	87	81

[a] Nucleotide position of B sequences showing highest similarity to GenBank sequences.
[b] Percentage identity of B to the GenBank sequence.
[c] The longest possible open reading frame (codon numbers).

presented in Table 6 (entries 14–16). pAFB1 (nt 1–500) and pAFB1E (nt 5–727), contiguous sequences with an overlap of 404 bp, had 89% (nt 68907–68407) and 91% (nt 69226–68504) identity, respectively, with a noncoding region upstream of the *rp*3-1 gene (GenBank accession no. AY574035) in chromosome 3. pAFB2 had 165 bp (nt 574-739) in common with the LTR of *Zeon*1a of the centromeric BAC ZM15C05 (nt 10007–9842, 87% identity; GenBank accession no. AC116033), and the remaining region had no appreciable similarity to any GenBank sequence. There is no homology between p3259 and p4049 and their respective flanking regions (<30% similarity). In addition, no trace of repetiveness—tandem or nontandem—exists within these three clones.

DISCUSSION

Thirteen sequences were cloned from B-derived AFLPs, which had been mapped to defined regions of the B chromosome by B-10L translocations. These regions cover euchromatic as well as heterochromatic portion. Two of these are nearly B specific, and the rest shared homology with the normal complements (A chromosomes).

Molecular characteristics of the B-derived AFLP sequences confirm those of AFLPs in general. When used as probe in genomic Southern analysis, 2 of 13 B clones displayed signals of discrete bands in a lightly smeared background (Figure 6, J and L), 3 displayed heavily smeared patterns (Figure 6, A, F, and I), and 8 others displayed discrete signals in a medium-smeared background (Figure 6, B, C, D, E, G, H, K, and M). Such Southern pattern is consistent with AFLP sequences of other plants. For example, 5 sex-linked clones of *Asparagus officinalis* L. showed more than six discrete bands in company with a smeared background, and their FISH signals dispersed all over the chromosomes (REAMON-BUTTNER *et al.* 1999). Similarly, sex-linked AFLP of *Rumex nivalis* (Polygonaceae) exhibited tandem arrangement and repetitive sequences (STEHLIK and BLATTNER 2003). Also repetitive were AFLP sequences of damselflies (WONG *et al.* 2001) and barley (MEKSEM *et al.* 1995).

The approach of cloning B sequences in this study is at variance with that of microdissection. In this study, 13 sequences were cloned from regions defined by the breakpoints of B-10L translocations, extending from the centromere to the distal region of the B large arm. On the contrary, the B sequences from microdissection were cloned randomly from cytological fragments of the B chromosome, whose chromosomal locations remain to be determined. Despite such topographical diversity, sequences obtained from the two sources are remarkably consistent: both are repetitive in nature, possess a high degree of homology to the A chromosomes, and have no similarity to any published gene other than fragments of retrotransposons. In addition,
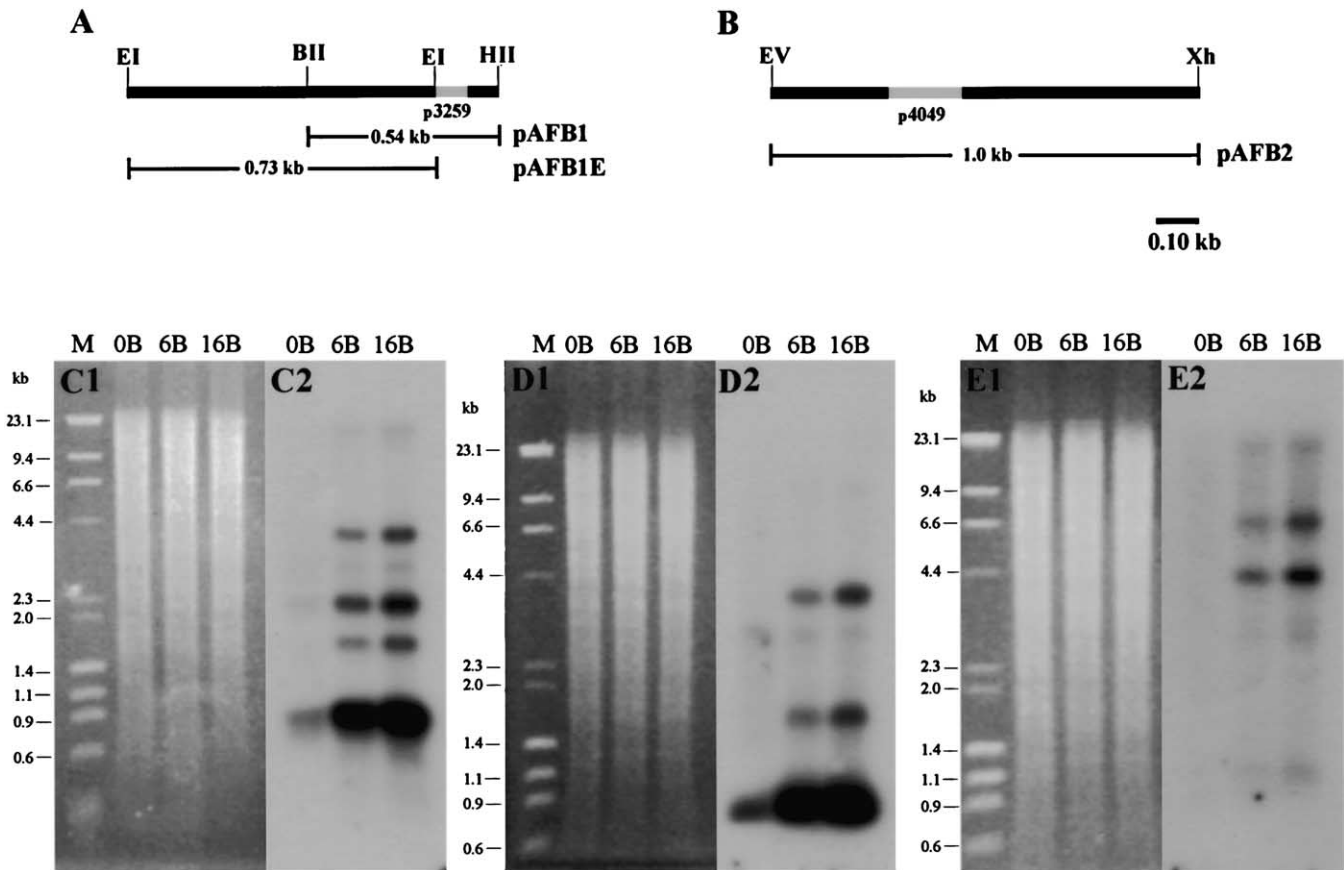
FIGURE 8.—Restriction maps and genomic organization of three B sequences associated with flanking regions of p3259 and p4049. (A) Restriction maps of pAFB1 and pAFB1E. (B) Restriction map of pAFB2. Genomic DNAs carrying 0, 6, and 16 B's were digested with *Eco*RI, stained with ethidium bromide (C1, D1, and E1), and probed with pAFB1 (C2), pAFB1E (D2), and pAFB2 (E2), respectively. EI, *Eco*RI; BII, *Bgl*II; HII, *Hinc*II; EV, *Eco*RV; and Xh, *Xho*I.

the two sources yielded B-exclusive sequence at low frequency, 2 of 13 clones in the former but 1 of 19 in the latter. However, minor differences between the two systems do exist. For example, the B-specific clones of the former (p3259 and p4049), when used as probe, produced only one to seven *Eco*RI bands (Figure 6, J and L), but that of the latter (pBPC51) produced a smeared signal (CHENG and LIN 2003). Also, microdissection resulted in more sequences displaying heavily smeared signals (18 of 19) than those derived from AFLP (8 of 13; Figure 6, A, C, E, F, G, H, I, and M). The excessive presence of high-copy sequences in microdissected B clones may have resulted from their screening procedure. Those B clones were uncovered by using the W22 + 16B DNA to probe the microdissected B library for identification of clones with positive signals. This screening procedure could have been biased against the low-copy sequence, which might express weak, undetectable signals.

Euchromatic and heterochromatic B regions displayed different molecular characteristics. Of the 13 sequences isolated in the current study, 3 are located in the proximal euchromatic region (PE) and 6 in the heterochromatic

regions (DH; the additional four are in regions proximal to TB-10L7 and the PE/DH1 junction). Clones from each region possessed their own distinctive Southern pattern. For example, DH contained two B-specific sequences (p4049 and p3259), but PE had none. Although both regions yielded hybridization types II, III, and IV (Table 4 and Figure 6), each sequence had its own characteristic pattern. No two sequences in the same or different regions are identical; they are different in either the number (and size) of discrete bands or the level of smeared background. Such distinctions also appear in the sequence characteristics (Table 6). Each region carried different retrotransposons; the euchromatic region contained the LTR of *Prem*-1 (p3850; entry 6, Table 6), the heterochromatic region the *gag* gene of Z*eon*1 (p3662$_2$; entry 9, Table 6) and the *pol* gene of *Xilon*2 (p4150$_2$; entry 13, Table 6)—an additional X*ilon*2 LTR-carrying clone (p3247$_1$; entry 7, Table 6). The only common feature between the two chromatins is their similarity to the centromeric BAC ZM15C05 (100 kb; GenBank accession no. AC116033; NAGAKI *et al.* 2003): p3850 in euchromatin and p3662$_2$ in heterochromatin.

Association of a 0.8-kb signal with p3259, pAFB1, and

pAFB1E is noteworthy, for it implies existence of a novel repeat in the B chromosome. The 0.8-kb signal appeared in the *Eco*RI digest of the W22 + 6B and W22 + 16B DNAs probed with each of the three clones (Figures 6L, 8C2, and 8D2). Its intensity is greater than that of any other signal of the same blot. For example, the 0.8-kb signal of p3259 is at least 5 times as intense as the 1.6-kb signal (Figure 6L). Appearance of such a prominent signal may indicate a repeat or part of two different repeat sequences carried by each of the p3259 and pAFB1E clones. Yet absence of any similarity between p3259 and pAFB1E in sequence analysis precludes this supposition. Thus, results are consistent with the notion of two independent repeats: one in p3259, the other in pAFB1E, and both in pAFB1. Accordingly, the lengths of the *Eco*RI fragments associated with the two repeats are coincidently equal. Alternatively, data can also be interpreted as having a single repeat in the B chromosome, extending from p3259 into part of pAFB1E, overlapping with the 5′ half of pAFB1. This notion is supported by the assumption that pAFB1 is an exceptional clone, carrying an internal *Eco*RI site, which is absent elsewhere in most regions of the B chromosome.

B chromosomes exist in both plant and animal kingdoms, but their origin is an enigma. On the basis of B characteristics, several origins have been proposed. The most popular view is that B chromosomes originated from the A chromosomes of the same species. For example, on the basis of their studies of the B and chromosome 4 centromere, Page *et al.* (2001) considered that the maize B chromosome is an aggregate of several A chromosomes. This notion is consistent with the microdissected B clones (Cheng and Lin 2003, 2004), whose sequences are correspondent to those of chromosomes 1, 4, 7, and 9. The sequence analyses of other plants also support this supposition, including *Crepis capillaries* (Jamilena *et al.* 1994), *Secale cereale* (Sandery *et al.* 1991), and Allium (Green 1990). Battaglia (1964) proposed that B chromosomes could arise through interspecific/intraspecific hybridization. This view was substantiated by Sapre and Deshpande (1987) who demonstrated that the B chromosome of *Coix aquaticus* resulted from interspecific crosses between *C. aquaticus* and *C. gigantean*. Finally, several observations suggest a possible role of sex chromosomes in the evolution of B chromosomes. For example, B sequences of the New Zealand frog *Leiopelma hochstetteri* from Great Barrier Island expressed homology to the univalent W sex chromosome of North Island populations (Sharbel *et al.* 1998). In this study, 10 of 13 B sequences displayed homology to the noncoding sequence of genomic clones carrying *rp3*-1, 22-kD *zein*, 19-kD *zein*, and *bz*1 and to BAC 163K15 (Ramakrishna *et al.* 2002) and centromeric BACs (ZM15C05 and ZM16H10), located on chromosomes 3, 4, 7, 9, and 10 as well as on

the centromere, respectively, consistent with the supposition of Page *et al.* (2001) and Cheng and Lin (2003, 2004).

LITERATURE CITED

Alfenito, M. R., and J. A. Birchler, 1993 Molecular characterization of a maize B chromosome centric sequence. Genetics **135:** 589–597.

Battaglia, E., 1964 Cytogenetics of B chromosomes. Caryologia **17:** 245–299.

Beckett, J. B., 1991 Cytogenetic, genetic and plant breeding applications of B-A translocations in maize, pp. 493–529 in *Chromosome Engineering in Plants: Genetics, Breeding Evolution*, Part A, edited by P. K. Gupta and T. Tsuchiya. Elsevier, Amsterdam.

Benson, G., 1999 Tandem repeats finder: a program to analyze DNA sequences. Nucleic Acids Res. **27:** 573–580.

Chen, C. C., C. M. Chen, J. T. Yang and Y. Y. Kao, 1998 Localization of a repetitive DNA sequence to the primary constrictions of maize pachytene chromosomes. Chromosome Res. **6:** 236–238.

Cheng, Y.-M., and B.-Y. Lin, 2003 Cloning and characterization of maize B chromosome sequences derived from microdissection. Genetics **164:** 299–310.

Cheng, Y.-M., and B.-Y. Lin, 2004 Molecular organization of large fragments in the maize B chromosome: indication of a novel repeat. Genetics **166:** 1947–1961.

Chung, C. T., S. L. Niemela and R. H. Miller, 1989 One-step preparation of competent *Escherichia coli*: transformation and storage of bacterial cells in the same solution. Proc. Natl. Acad. Sci. USA **86:** 2172–2175.

Cnops, G., B. Den Boer, A. Gerats, M. Van Montagu and M. Van Lijseberttens, 1996 Chromosome landing at the *Arabidopsis TORNADO*1 locus using an AFLP-based strategy. Mol. Gen. Genet. **253:** 32–41.

Green, D. M., 1990 Muller's ratchet and the evolution of supernumerary chromosomes. Genome **33:** 818–824.

Jamilena, M., C. R. Rejón and M. R. Rejón, 1994 A molecular analysis of the origin of the *Crepis capillaris* B chromosome. J. Cell Sci. **107:** 703–708.

Kaszás, É., and J. A. Birchler, 1996 Misdivision analysis of centromere structure in maize. EMBO J. **15:** 5246–5255.

Lin, B.-Y., 1978 Regional control of nondisjunction of the B chromosome in maize. Genetics **90:** 613–627.

Lin, B.-Y., 1979 Two new B-10 translocations involved in the control of nondisjunction of the B chromosome in maize. Genetics **92:** 931–945.

Lin, B.-Y., and H.-P. Chou, 1997 Physical mapping of four RAPDs in the B chromosome of maize. Theor. Appl. Genet. **94:** 534–538.

Lin, B.-Y., S.-F. Peng, Y.-J. Chen, H.-S. Chen and C.-F. Kao, 1997 Physical mapping of RFLP markers on four chromosome arms in maize using terminal deficiencies. Mol. Gen. Genet. **256:** 509–516.

McClintock, B., 1933 The association of non-homolog parts of chromosome in the mid-prophase of meiosis of *Zea mays*. Zeitschr. Zellforsch. **19:** 191–237.

Meksem, K., D. Leister, J. Peleman, M. Zabeau, F. Salamini *et al.*, 1995 A high-resolution map of the vicinity of the *R*1 locus on chromosome V of potato based on RFLP and AFLP markers. Mol. Gen. Genet. **249:** 74–81.

Nagaki, K., J. Song, R. M. Stupar, A. S. Parokonny, Q. Yuan *et al.*, 2003 Molecular and cytological analyses of large tracks of centromeric DNA reveal the structure and evolutionary dynamics of maize centromeres. Genetics **163:** 759–770.

Page, B. T., M. K. Wanous and J. A. Birchler, 2001 Characterization of a maize chromosome 4 centromeric sequence: evidence for an evolutionary relationship with the B chromosome centromere. Genetics **159:** 291–302.

Ramakrishna, W., J. Emberton, M. Ogden, P. Sanmiguel, J. L. Bennetzen *et al.*, 2002 Structural analysis of the maize *Rp*1 complex reveals numerous site and unexpected mechanisms of local rearrangement. Plant Cell **14:** 3213–3223.

Randolph, L. F., 1941 Genetic characteristics of the B chromosomes in maize. Genetics **26:** 608–631.

Reamon-Buttner, S. M., T. Schmidt and C. Jung, 1999 AFLPs

represent highly repetitive sequences in *Asparagus officinalis* L. Chromosome Res. **7:** 297–304.

SANDERY, M. J., J. W. FORSTER, S. R. MACADAM, R. BLUNDEN, R. N. JONES *et al.*, 1991 Isolation of a sequence common to A- and B- chromosomes of rye (*Secale cereale*) by microcloning. Plant Mol. Biol. Rep. **9:** 21–30.

SAPRE, A. B., and D. S. DESHPANDE, 1987 Origin of B chromosome in *Coix* L. through spontaneous interspecific hybridization. J. Hered. **78:** 191–196.

SHARBEL, T. F., D. M. GREEN and A. HOUBEN, 1998 B-chromosome origin in the endemic New Zealand frog *Leiopelma hochstetteri* through sex chromosome devolution. Genome **41:** 14–22.

STARK, E. A., I. CONNERTON, S. T. BENNETT, S. R. BARNES, J. S. PARKER *et al.*, 1996 Molecular analysis of the structure of the maize B-chromosome. Chromosome Res. **4:** 15–23.

STEHLIK, I., and F. R. BLATTNER, 2003 Sex-specific SCAR markers in the dioecious plant *Rumex nivalis* (Polygonaceae) and implications for the evolution of sex chromosomes. Theor. Appl. Genet. **108:** 238–242.

TATUSOVA, T. A., and T. L. MADDEN, 1999 Blast 2 sequences—a new tool for comparing protein and nucleotide sequences. FEMS Microbiol. Lett. **174:** 247–250.

VOS, P., R. HOGERS, M. BLEEKER, M. REIJANS, T. VAN DE LEE *et al.*, 1995 AFLP: a new technique for DNA fingerprinting. Nucleic Acids Res. **23:** 4407–4414.

VUYLSTEKE, M., R. MANK, R. ANTONISE, E. BASTIAANS, M. L. SENIOR *et al.*, 1999 Two high-density AFLP linkage maps of *Zea mays* L.: analysis of distribution of AFLP markers. Theor. Appl. Genet. **99:** 921–935.

WONG, A., M. R. FORBES and M. L. SMITH, 2001 Characterization of AFLP markers in damselflies: prevalence of codominant markers and implications for population genetic applications. Genome **44:** 677–684.

XU, M., E. HUARACHA and S. S. KORBAN, 2001 Development of sequence-characterized amplified regions (SCARs) from amplified fragment length polymorphism (AFLP) markers tightly linked to the *Vf* gene in apple. Genome **44:** 63–70.

Communicating editor: J. A. BIRCHLER